Available online at www.sciencedirect.com

SciVerse ScienceDirect

Ceramics International 39 (2013) 6805–6811

CERAMICS INTERNATIONAL

www.elsevier.com/locate/ceramint

Growth behavior of nanosized ceria powders prepared by coprecipitation routes

GuoLi Yang[a,1], Horng-Huey Ko[b], Yu-Wei Hsu[c], Ko-Ho Yang[c], Moo-Chin Wang[b,*], Jianjun Han[a], Xiu Jian Zhao[a,**]

[a]State Key Laboratory of Silicate Materials for Architectures (Wuhan University of Technology), Wuhan 430070, People's Republic of China
[b]Department of Fragrance and Cosmetic Science, Kaohsiung Medical University, 100 Shih-Chuan 1st Road, Kaohsiung 80708, Taiwan
[c]Graduate Institute of Applied Science, National Kaohsiung University of Applied Sciences, 415 Chien-Kung Road, Kaohsiung 80782, Taiwan

Received 13 December 2012; received in revised form 5 February 2013; accepted 5 February 2013
Available online 13 February 2013

Abstract

Nanosized ceria (CeO_2) powders were obtained by coprecipitation routes of cerium nitrate hexahydrate [$Ce(NO_3)_3 \cdot 6H_2O$]. The growth behavior of the nanosized CeO_2 powders was investigated by X-ray diffraction, transmission electron microscopy and selected area electron diffraction. The XRD results showed that the dried precursor powders contained a single crystalline phase of CeO_2, and only a single phase of CeO_2 appeared when the dried precursor powders were calcined at different temperatures for various durations. Moreover, the crystallite size of CeO_2 increased on increasing the calcination temperature and duration. The kinetics equation of the nanosized CeO_2 powders grown between 673 and 1273 K for various durations is described as

$D_t - D_0 = kt^m \exp(-56.42 \times 10^3/RT)$ where $k = 7.5 \times 10^{-1}$ and $m = 0.20$ when $t \leq 360$ min and 673 K $\leq T \leq$ 873 K; $k = 8.46$ and $m = 0.43$ when 5 min $\leq t \leq$ 30 min and 1073 K $\leq T \leq$ 1273 K; and $k = 3.17 \times 10$ and $m = 0.03$ when 30 min $\leq t \leq$ 360 min and 1073 K $\leq T \leq$ 1273 K.

Keywords: Ceria; Coprecipitation powders; Kinetic equation

1. Introduction

In recent years, materials based on ceria (CeO_2) have been extensively studied owing to their potential for use in a wide range of applications such as solid oxide fuel cells [1,2], gas sensors [3], photocatalytic oxidation of water [4,5], UV absorbents and filters [6,7]. The practical performance of such materials is strongly influenced by the properties of their constituents and the size of the CeO_2 particles.

Over the past few years, numerous techniques such as hydrothermal [8,9], sol–gel [10], microwave [11], microemulsion [12], reverse micelles [13], and homogeneous precipitation [14–17] have been widely used to synthesize nanosized CeO_2 particles in a way that offers large control of their properties. Among these techniques, homogeneous precipitation is one of the most promising because of low cost, easy-to-acquire apparatus, a simple synthesis process, and nanometric precursor particles. Zhou et al. [14] used room-temperature homogenous nucleation to synthesize thermally stable CeO_2 from cerium nitrate ammonia in which the average size of a single CeO_2 crystal was 4 nm. Uekawa et al. [15] also reported that 7–9 nm CeO_2 spherical fine particles were obtained using cerium nitrate as the starting materials for their homogenous precipitation in a polyethylene glycol (PEG) solution. Zhang et al. [16] reported the synthesis of cerium rhombic microplates via ultrasonication using PEG as a structure-directing agent prepared at room temperature. They obtained nanorods of polycrystalline CeO_2 that had a diameter of 5–10 nm and length of 50–150 nm. Hassanzadeh-Tabrizi et al. [17] proposed that the activation

*Corresponding author. Tel.: +886 7 3121101x2366.
**Corresponding author. Tel.: +86 13871110463.
E-mail addresses: mcwang@kmu.edu.tw (M.-C. Wang), opluse@whut.edu.cn (X.J. Zhao).
[1]Present address: Teching and Research Section for Mechanical Foundation, Foundation Department, Wuhan Ordnance N.C.O Academy P.L.A. Luoyu Road No. 1038, Wuhan 430075, P.R. China

0272-8842/$ - see front matter © 2013 Elsevier Ltd and Techna Group S.r.l. All rights reserved.
http://dx.doi.org/10.1016/j.ceramint.2013.02.011

energy for the growth of CeO_2 nanopowder was 14.6 kJ/mol for a precursor obtained via reverse precipitation synthesis.

El-Adham and Gadalla [18] pointed out that the activation energy of CeO_2 crystallite growth depends on the type of CeO_2 precursor used. Using X-ray powder diffraction to investigate the growth kinetics of nanosized CeO_2 crystallites prepared from ceric ammonium and sulfate salts, Audebrand et al. [19] also found that the activation energy and growth rate of CeO_2 crystallites depend on the precursor used.

With regard to the preparation of CeO_2 nanoparticles, although the precipitation technique has been widely used, most related studies have focused on the effects of cerium precursors, ligands, additives, and reaction media on the process. However, the effects of calcination temperature on the crystallite growth behavior of dried ceria precursor powder obtained by a coprecipitation process have not yet been elaborated in the literature.

In the present study, the growth behavior of nanosized ceria powders obtained by coprecipitation routes of cerium nitrate hexahydrate [$Ce(NO_3)_3 \cdot 06H_2O$] was investigated. The characteristic growth behavior of the nanosized CeO_2 powders was studied by X-ray diffraction (XRD), transmission electron microscopy (TEM), and selected area electron diffraction (SAED). The following are the aims of this investigation: (i) study the growth behavior of CeO_2 powders as produced by calcination; (ii) evaluate the activation energy and kinetics of CeO_2 crystallite growth; and (iii) examine the TEM microstructure of both uncalcined and calcined CeO_2 powders.

2. Experimental procedures

2.1. Sample preparation

$Ce(NO_3)_3 \cdot 6H_2O$ (purity $\geq$ 99.0%, supplied by Sinopharm Chemical Reagent Co., Ltd., China) was used in this study as the starting material. PEG (M_W=600, supplied by Sinopharm Chemical Reagent Co., Ltd., China) was used as a dispersant. $Ce(NO_3)_3 \cdot 6H_2O$ was dissolved in a solution of deionized water and ethanol at a volume ratio of 4:1. A concentration of $Ce(NO_3)_3$ equal to 0.1 mol/L in solution was prepared and 1 wt% PEG as a dispersion agent was added to reduce the agglomeration. The mixed solution was stirred by a magnetic stirrer at 293 K. NH_4OH (supplied by Sinopharm Chemical Reagent Co., Ltd., China) was then gradually added to the solution until a pH of 9 was obtained. After precipitation, the precipitates were repeatedly rinsed with large amounts of deionized water and ethanol. Subsequently, the precursor powders were oven-dried at 313 K. Finally, the dried precursor powders were calcined at different temperatures for various durations.

2.2. Sample characterization

The crystalline phase was identified by XRD (Rigaku-D/MAX-RB X-ray, Tokyo) with Cu Kα radiation and a Ni filter operating at 40 kV and 50 mA, with a scanning rate (2θ) of 1°/min. The average crystallite size of the ceria dried precursor powders calcined at different temperatures for various durations was calculated using the Scherrer equation [20]

$$D_{hkl} = \frac{0.89\lambda}{\beta \cos\theta} \quad (1)$$

where D_{hkl} denotes the average crystallite size of the CeO_2 (h k l) reflection peak, λ=0.15405 nm is the X-ray wavelength of Cu Kα, β is the full-width at half maximum intensity (FWHM), and θ is the Bragg's angle of the peak.

The morphology of the uncalcined ceria dried precursor powders and calcined samples was examined by TEM (Tecnai G20, FEI Co., USA) with SAED operating at 200 kV.

3. Results and discussion

3.1. Crystallite structure and size of CeO_2

The XRD patterns of the ceria dried precursor powders calcined at various temperatures for 360 min are shown in Fig. 1. The reflection peaks of (1 1 1), (2 0 0), (2 2 0), and (3 1 1) are seen, which correspond to CeO_2. This result is attributed to the presence of a single crystalline phase of CeO_2 in the dried precursor powders. However, the broad and weak intensities of the peaks indicate fine crystallites and poor crystallinity of CeO_2. When the calcination temperature was increased to 873 K, the XRD patterns remained the same, showing the same broad and weak peaks. This is because the CeO_2 powders still maintain the same fine crystallites and poor crystallinity. However, when calcination temperature was increased from 873 K to 1073 K and 1273 K, the reflection peaks became sharper and stronger, indicating that the crystallite size increased and the crystallinity improved in the CeO_2 powders.

Fig. 2 shows the crystallite size of the CeO_2 dried precursor powders calcined at different temperatures for

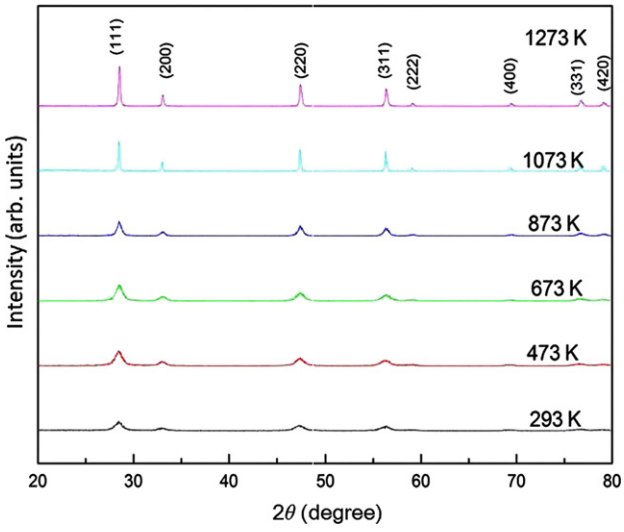

Fig. 1. XRD patterns of ceria dried precursor powders calcined at various temperatures for 360 min.

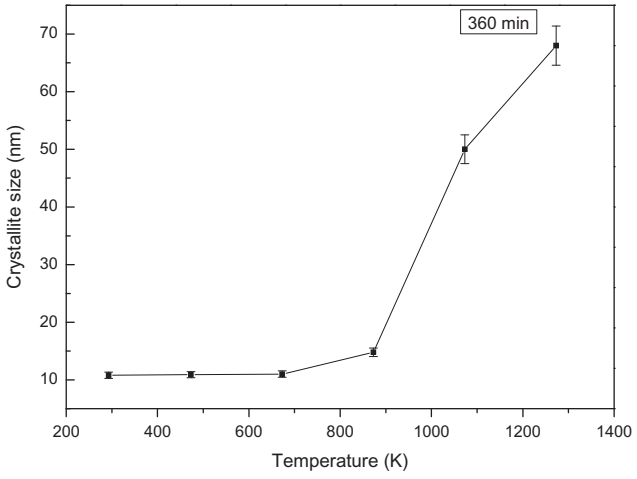

Fig. 2. Average crystallite sizes of the ceria dried precursor powders calcined at different temperatures for 360 min.

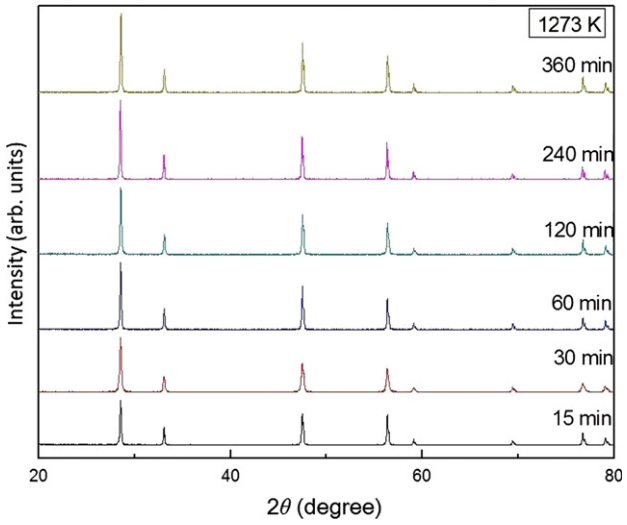

Fig. 3. XRD patterns of ceria dried precursor powders calcined at 1273 K for various durations.

360 min based on the XRD line-broadening of the (1 1 1) reflection peak. The figure shows that the change in the crystallite size of CeO_2 is minimal at the calcination temperatures ≦673 K. However, the crystallite size increases at the calcination temperatures ≧873 K. Li et al. [21] noted that the crystallite size of CeO_2 shows an exponential dependence on the calcination temperature because the crystallite growth of CeO_2 is controlled by diffusion.

Fig. 2 also shows that the crystallite sizes of the ceria dried precursor powders calcined at 473 K and 873 K for 360 min are 11.0 and 14.8 nm, respectively. These results reveal that the crystallite growth is very slow at the calcination temperatures ≦873 K. However, when the ceria dried precursor powders were calcined at 1273 K for 60 min, the crystallite size rapidly increased to 67.9 nm. Continuous grain boundary networks are formed at the calcination temperatures ≧873 K. These networks lead to the bridging of fine crystallites, thereby increasing the crystallite size.

Fig. 3 shows the XRD patterns of the ceria dried precursor powders calcined at 1273 K for various durations. The figure shows that the broadening of the CeO_2 reflections disappears because of the crystallite growth. Moreover, the intensity of the CeO_2 (1 1 1) reflection increases with increase in the calcination duration as a result of increasing crystallinity. In addition, the XRD patterns of the ceria dried precursor powders calcined at different temperatures for various durations are similar to those in Fig. 3. The difference between these is that only the broadening reflection peaks exist for calcination at lower temperature for shorter durations.

The crystallite sizes of the ceria dried precursor powders calcined at fixed temperatures for various durations are shown in Fig. 4. During calcination between 873 and 1273 K, the crystallite size increased only slightly on increasing the calcination duration. At 873 K, the crystallite size increased only slightly, from 10.0 to 10.9 nm (a 9% increase), when the duration was increased from 5 to 360 min. When calcined at 873 K for 5 and 360 min, the crystallite sizes were 11.7 and 14.8 nm, respectively. However, when the dried precursor powders were calcined at 1073 K, the crystallite size increased rapidly from 18.1 nm at 5 min to 40.5 nm at 60 min. The crystallite size then increased only slightly from 40.5 at 60 min to 50.0 nm at 360 min. Thus, at calcination temperatures ≧873 K, the crystallite size increases rapidly with increase in duration from 5 to 60 min. These results suggest that the pores existing in the interior of the ceria dried precursor powders are rapidly eliminated under these conditions.

3.2. Kinetics of CeO_2 nanocrystallite growth

To determine the activation energy of the nanocrystallite growth of ceria dried precursor powders calcined at various temperatures for different durations, the general equation for the kinetics of isothermal crystallite growth is

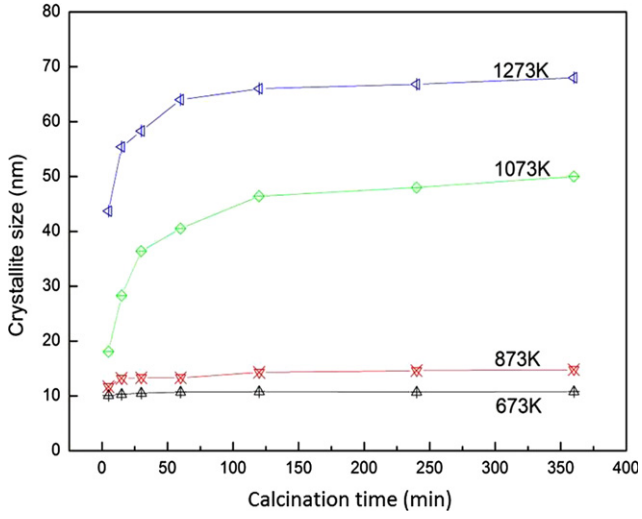

Fig. 4. Average crystallite sizes of ceria dried precursor powders as calcined at different temperatures for various durations.

described as follows [22]:

$$D_t^n - D_0^n = Gt^m \quad (2)$$

where n is a constant for a given growth mechanism, D_t is the crystallite size at time t, D_0 is a reference crystallite size at initial time t_0, G is a temperature dependent constant, and m is the time exponent.

The value $n=1$ represents anomalous narrow crystal growth, whereas $n=2$ suggests normal crystallite growth. A value of $n=3$ shows solid-solution-drag-controlled crystallite growth, and $n=4$ denotes pore-drag-controlled crystallite growth [23].

Fig. 1 shows that ceria dried precursor powders at room temperature (293 K) contained only a single crystalline phase of CeO_2; therefore, the initial time can be assumed to be $t_0=0$. Fig. 4 shows that the anomalous crystallite growth behavior of the ceria dried precursor powders is caused by the presence of pores in the interface regions of the CeO_2 powders [23]. Therefore, the growth kinetics equation can be fitted with $n=1$ and described as follows (3)

$$D_t - D_0 = Gt^m \quad (3)$$

The temperature-dependent constant G can be expressed by [22]

$$G = k\exp\left(-\frac{\Delta E}{RT}\right) \quad (4)$$

where k is a pre-exponential factor, R denotes the gas constant, T is the absolute temperature and ΔE is the activation energy for crystallite growth.

Combining Eqs. (3) and (4) gives

$$D_t - D_0 = kt^m\, e^{-(\Delta E/RT)} \quad (5)$$

Taking the logarithm of both left hand side and right hand side of Eq. (5) gives

$$\ln(D_t - D_0) = \ln k + m\ln t - \frac{\Delta E}{RT} \quad (6)$$

The relation between $\ln(D_t-D_0)$ and $1/T$ of the CeO_2 dried precursor powders calcined at various temperatures for different durations is shown in Fig. 5. The apparent average activation energy of CeO_2 crystallite growth, 56.42 kJ/mol, can be calculated from the slopes.

The dependence of $\ln(D_t-D_0)$ on $\ln t$ of the ceria dried precursor powders calcined at 673 and 873 K for various durations is shown in Fig. 6. Based on the calculation from the slopes, the value of the average time exponent (m) is obtained as 0.2. If we let $\ln t \to 0$, then the average value of $k=7.5\times10^{-1}$ is also obtained.

For the ceria dried precursor powders calcined at 1073 and 1273 K for 5 and 30 min, respectively, Fig. 6 shows the plots of $\ln(D_t-D_0)$ against $\ln t$. The values of the parameters m and k, as 0.43 and 8.46, respectively, are obtained by Eq. (6) for the calculated CeO_2 crystallite growth. In addition, Fig. 6 shows the plots of $\ln(D_t-D_0)$ versus $\ln t$ when the ceria dried precursor powders were calcined at 1073 and 1273 K for duration longer than 30 min. In this case, the values of m and k are approximately 0.03 and 3.17×10, respectively.

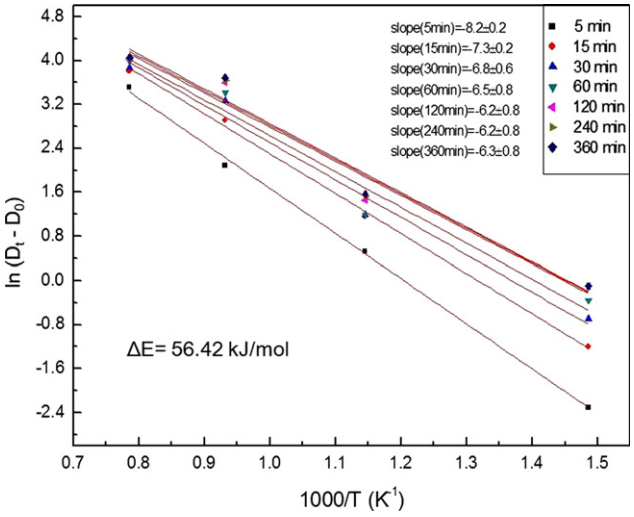

Fig. 5. $\ln(D_t-D_0)$ versus $1/T$.

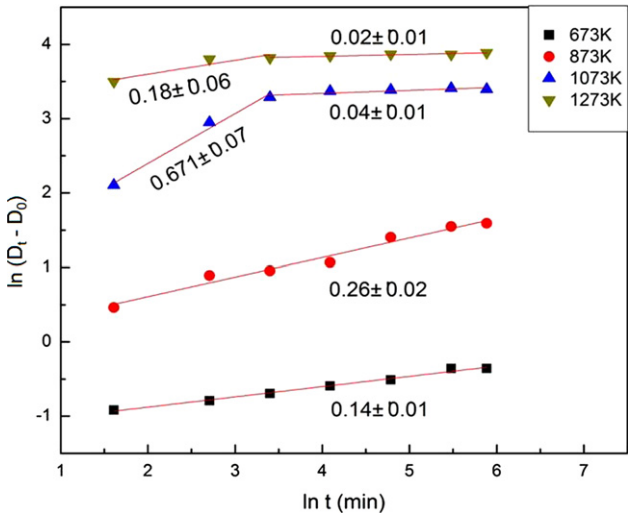

Fig. 6. Relation between $\ln(D_t-D_0)$ and $\ln t$ for ceria dried precursor powder calcined at various temperatures.

The growth kinetics equation of CeO_2 from dried precursor powders are thus described by

$$D_t - D_0 = kt^m \exp\left(-\frac{56.42\times10^3}{RT}\right) \quad (7)$$

where $k=7.5\times10^{-1}$ and $m=0.20$ when $t\le360$ min and 673 K $\le T\le$ 873 K; $k=8.46$ and $m=0.43$ when 5 min $\le t\le$ 30 min and 1073 K $\le T\le$ 1273 K; and $k=3.17\times10$ and $m=0.03$ when 30 min $\le t\le$ 360 min and 1073 K $\le T\le$ 1273 K.

The average apparent activation energy in the present study is 56.42 kJ/mol, which is close to 48.7 kJ/mol of the nanocrystallite CeO_2 growth from the thermal decomposition of cerous nitrate [20]. In addition, the activation energy of the present result is higher than the value

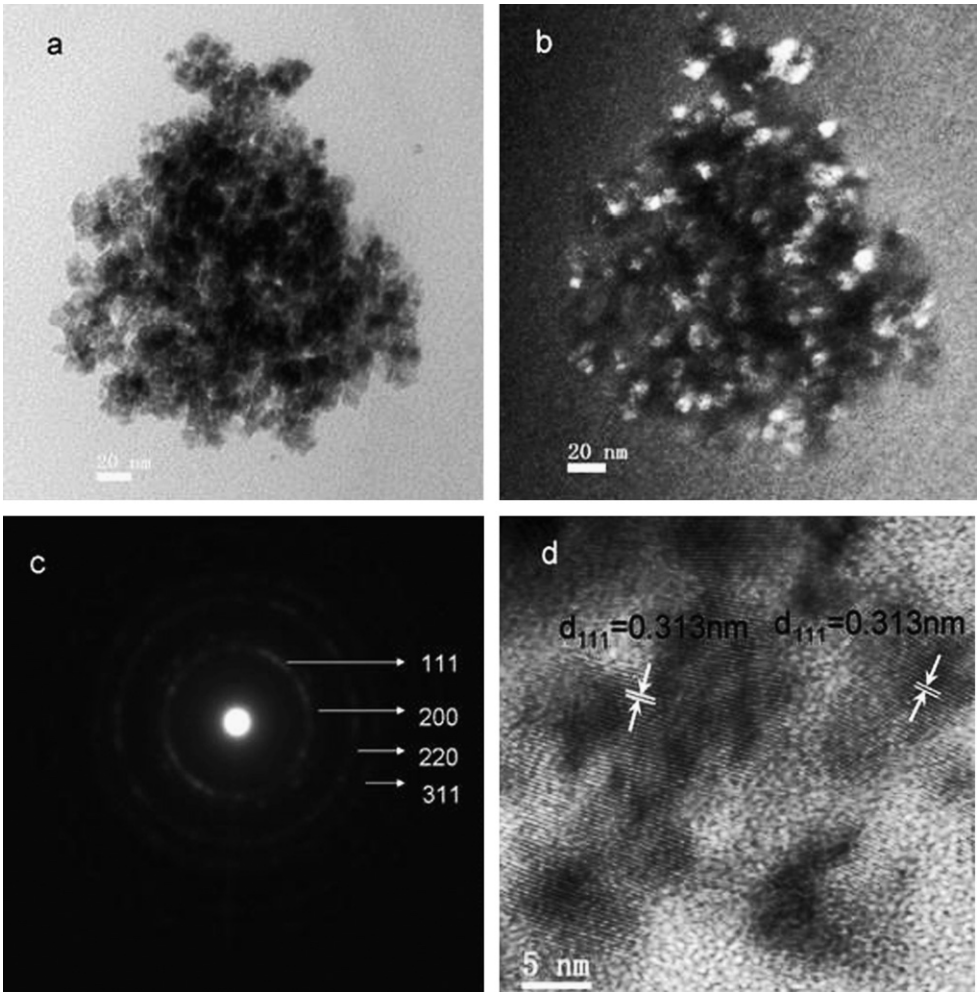

Fig. 7. TEM microstructures of ceria dried precursor powders before calcinations: (a) BF image, (b) DF image, (c) SAED pattern indexed corresponding to CeO_2, and (d) high resolution TEM image of the CeO_2 with d_{111}=0.313 nm.

14.6 kJ/mol reported by Hassanzadeh-Tabrizi et al. [17], but lower than 157 and 231 kJ/mol for CeO_2 crystallite growth obtained from sulfate and ammonium salts, respectively [19]. These results could be owing to the various rates of crystallite growth for the different precursors and various processes [17–19].

The low activation energy found in the present study supports the claim that bulk nucleation is dominant in CeO_2 crystallization and that the crystallite growth is controlled by the diffusion of the crystallite boundaries or lattices.

3.3. Microstructure of ceria dried precursor powders before and after calcination

The bright field (BF) and dark field (DF) TEM microstructures of the ceria dried precursor powders before calcination are shown in Fig. 7(a) and (b), respectively, which show an ultrafine primary particle size of about 10 nm. This result is in agreement with the particle size calculated from the XRD results. Fig. 7(c) shows the SAED pattern, which is indexed corresponding to CeO_2. This result also provides evidence for a single crystalline phase of CeO_2 in the dried precursor powders, and it agrees with the clear XRD reflection peak of the ceria dried precursor powder. Fig. 7(d) shows the high-resolution TEM (HR-TEM) image of the CeO_2 nanocrystallite, in which the *d*-spacing of CeO_2 (1 1 1) is 0.313 nm, as indicated by the arrows.

Fig. 8 shows the TEM microstructure, SAED pattern, and HR-TEM image of the ceria dried precursor powder calcined at 1273 K for 60 min. Fig. 8(a) and (b) shows the BF and DF images, respectively, which reveal many crystallites with sizes of 68 nm. According to Fig. 4(b), the crystallite size observed by TEM agrees with the result obtained using the Scherrer formula (Eq. (1)). Fig. 8(c) shows the SAED pattern, which is indexed corresponding to CeO_2. The HR-TEM image of the ceria dried precursor powders as calcined at 1273 K for 60 min is shown in Fig. 7(d). The *d*-spacing of CeO_2 in the [1 1 1] direction and that of CeO_2 (1 1 1) is 0.310 nm.

4. Conclusion

The growth behavior of nano-sized CeO_2 powders was investigated by XRD, TEM, and SAED. The XRD results

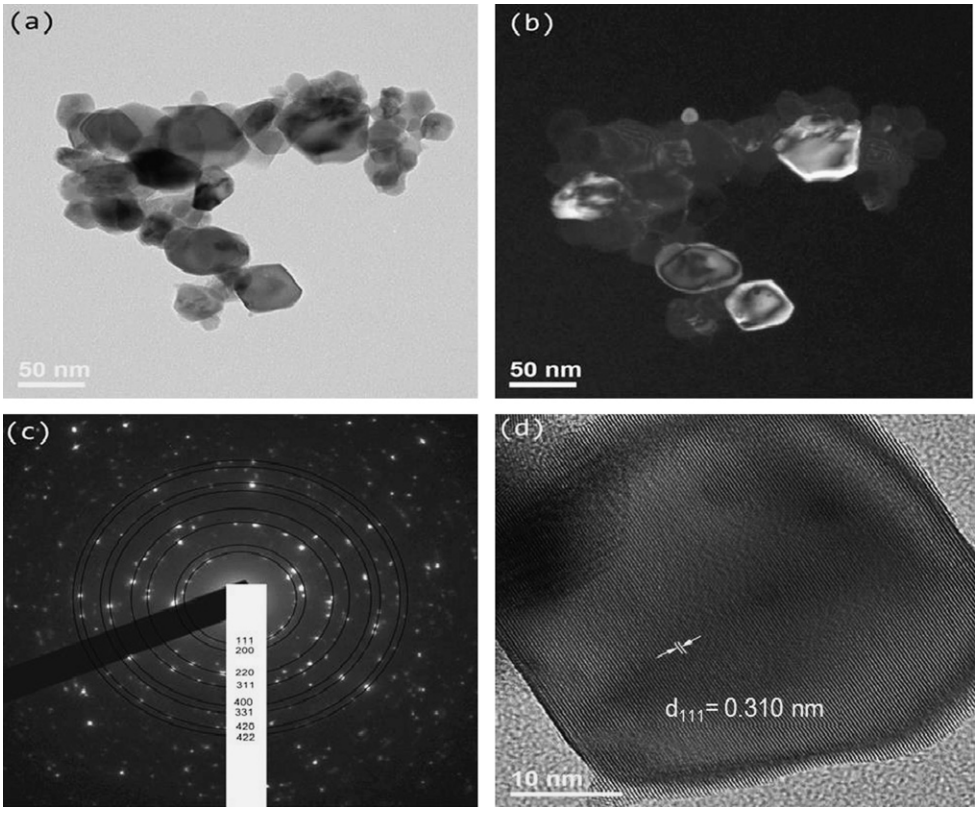

Fig. 8. TEM microstructure of ceria dried precursor powders calcined at 1273 K for 60 min: (a) BF image, (b) DF image, (c) SAED pattern indexed corresponding to CeO_2, and (d) high resolution TEM image of the CeO_2 in Fig. 8(b), indicated by arrow showing $d_{111}=0.310$ nm.

show that the dried precursor powder contained only a single crystalline phase of CeO_2 but had poor crystallinity. When the dried precursor powders were calcined at various temperatures for different durations, the powders still contained only a single phase of CeO_2. However, the crystallinity and crystallite size of CeO_2 increased with increase in the calcination temperature and duration. The activation energy of CeO_2 crystallite growth was determined as 56.42 kJ/mol. For dried precursor powders calcined at various temperatures for different durations, the kinetics equation of CeO_2 crystallite growth is expressed as follows:

$$D_t - D_0 = kt^m \exp(-\frac{56.42 \times 10^3}{RT})$$

where $k=7.5\times10^{-1}$ and $m=0.20$ when $t\le360$ min and 673 K $\le$ T $\le$ 873 K; $k=8.46$ and $m=0.43$ when 5 min $\le t\le30$ min and 1073 K $\le T\le$ 1273 K; and $k=3.17\times10$ and $m=0.03$ when 30 min $\le t\le360$ min and 1073 K $\le T\le$ 1273 K.

Acknowledgments

The authors gratefully acknowledge the financial support by the National Basic Research Program of China (2009CB939704), Natural Science Foundation of China (No. 51032005), and the Fundamental Research Funds for the Central Universities (Wuhan University of Technology). They also thank LinQing Qin for assistance with the XRD analysis (Wuhan University of Technology), as well as JinZhao Wang (Hubei University) and Mr. Shyue-Yen Yau (National Cheng Kung University, Taiwan) for the TEM experimentation during the preparation of this paper.

References

[1] A. Ainirad, M.M.K. Motlagh, A. Maghsoudipoor, A systematic study on the synthesis of Ca, Gd codoped cerium oxide by combustion method, Journal of Alloys and Compounds 509 (2011) 1505–1510.
[2] Y.P. Fu, Y.C. Liu, S.H. Hu, Aqueous tape casting and crystallization behavior of gadolinium-doped cerium dioxide, Ceramics International 35 (2009) 3153–3159.
[3] N. Izu, W. Shin, N. Murayama, S. Kanzaki, Resistive oxygen gas sensors based on CeO_2 fine powder prepared using mist pyrolysis, Sensors and Actuators B: Chemical 87 (2002) 95–98.
[4] J.K. Reddy, G. Suresh, C.H. Hymavathi, V.D. Kumari, M. Subrahmanyam, Ce(III) species supported zeolites as novel photocatalysts for hydrogen production from water, Catalysis Today 141 (2009) 89–93.
[5] Y.Z. Li, Q. Sun, M. Kong, W.Q. Shi, J.C. Huang, J.W. Tang, X.J. Zhao, Coupling oxygen ion conduction to photocatalysis in mesoporous nanorod-like cerium dioxide significantly improves photocatalytic efficiency, Journal of Physical Chemistry C 115 (2011) 14050–14057.
[6] S. Tsunekawa, R. Sahara, Y. Kawazoe, A. Kasuya, Origin of the blue shift in ultraviolet absorption spectra of nanocrystalline CeO_2 particles, Material Transactions, JIM 41 (2000) 1104–1107.

[7] S. Yabe, M. Yamashita, S. Momose, K. Tahira, Synthesis and UV-shielding properties of metal oxide doped cerium dioxide via soft solution chemical processes, International Journal of Inorganic Materials 3 (2001) 1003–1008.
[8] A.I.Y. Tok, F.Y.C. Boey, Z. Dong, X.L. Sun, Hydrothermal synthesis of CeO_2 nano-particles, Journal of Materials Processing Technology 190 (2007) 217–222.
[9] S.K. Sahoo, M. Mohapatra, A.K. Singh, S. Anand, Hydrothermal synthesis of single crystalline nano CeO_2 and its structural, optical, and electronic characterization, Materials and Manufacturing Processes 25 (2001) 982–989.
[10] S. Pavasupreea, Y. Suzukia, S. Pivsa-Artb, S. Yoshikawaa, Preparation and characterization of mesoporous MO_2 (M = Ti, Ce, Zr, and Hf) nanopowders by a modified sol–gel method, Ceramics International 31 (2005) 959–963.
[11] H. Yang, C. Huang, A. Tang, X. Zhang, W. Yang, Microwave-assisted synthesis of cerium dioxide nanoparticles, Materials Research Bulletin 40 (2005) 1690–1695.
[12] J. Zhang, X. Ju, Z.Y. Wu, T. Liu, T.D. Hu, Y.N. Xie, Structural characteristics of cerium oxide nanocrystals prepared by the micro-emulsion method, Chemistry of Materials 13 (2001) 4192–4197.
[13] S. Sathyamurthy, K.J. Leonard, R.T. Dabestani, M.P. Paranthaman, Reverse micellar synthesis of cerium oxide nanoparticles, Nanotechnology 16 (2005) 1960–1964.
[14] X.D. Zhou, W. Huebner, H.U. Anderson, Room-temperature homogeneous nucleation synthesis and thermal stability of nanometer single crystal CeO_2, Applied Physics Letters 80 (2002) 3814–3816.
[15] N. Uekawa, M. Ueta, Y.J. Wu, K. Kakegawa, Synthesis of CeO_2 spherical fine particles by homogeneous precipitation method with polyethylene glycol., Chemistry Letters 8 (2002) 854–855.
[16] D.S. Zhang, J.P. Zhang, L.Y. Shi, Facile synthesis of cerium dioxide rhombic microplates, Journal of Materials Science 43 (2008) 5647–5650.
[17] S.A. Hassanzadeh-Tabrizi, M. Mazaheri, M. Aminzare, S.K. Sadrnezhaad, Reverse precipitation synthesis and characterization of CeO_2 nanopowder, Journal of Alloys and Compounds 497 (2010) 499–502.
[18] K.A. El-Adham, A.M.M. Gadalla, Decomposition of some cerium salts and crystallite size of ceric oxide produced, Interceram 3 (1977) 223–226.
[19] N. Audebrand, J.P. Auffrédic, D. Louër, An X-ray powder diffraction study of the microstructure and growth kinetics of nanoscale crystallites obtained from hydrated cerium oxides, Chemistry of Materials 12 (2000) 1791–1799.
[20] B.D. Cullity, Elements of X-Ray Diffraction, second ed., Addison-Wesley Publishing Company, Reading, MA, 1978 99–102.
[21] J.G. Li, T. Ikegami, J.H. Lee, T. Mori, Characterization and sintering of nanocrystalline CeO_2 powders synthesized by a mimic alkoxide method., Acta Materialia 49 (2001) 419–426.
[22] G. Li, L. Li, J. Boerio-Goates, B.F. Woodfield, High purity anatase TiO_2 nanocrystals: near room-temperature synthesis, grain growth kinetics, and surface hydration chemistry, Journal of the American Chemical Society 127 (2005) 8659–8666.
[23] J.K.L. Lai, C.H. Shek, G.M. Lin, Grain growth kinetics of nanocrystalline SnO_2 for long-term isothermal annealing, Scripta Materialia 49 (2003) 441–446.